Title

Normative brain size variation and brain shape diversity in humans

Journal

Science, 360(6394)

ISSN

0036-8075

Authors

Reardon, PK
Seidlitz, Jakob
Vandekar, Simon
et al.

Publication Date

2018-06-15

DOI

10.1126/science.aar2578

Peer reviewed

Published in final edited form as:

Science. 2018 June 15; 360(6394): 1222–1227. doi:10.1126/science.aar2578.

Normative brain size variation and brain shape diversity in humans

P. K. Reardon[1,2,3,*], **Jakob Seidlitz**[1,4,*], **Simon Vandekar**[5], **Siyuan Liu**[1], **Raihaan Patel**[6,7], **Min Tae M. Park**[6,8], **Aaron Alexander-Bloch**[9], **Liv S. Clasen**[1], **Jonathan D. Blumenthal**[1], **Francois M. Lalonde**[1], **Jay N. Giedd**[10], **Ruben C. Gur**[11], **Raquel E. Gur**[11], **Jason P. Lerch**[12], **M. Mallar Chakravarty**[6,7], **Theodore D. Satterthwaite**[11], **Russell T. Shinohara**[5], **Armin Raznahan**[1,†]

[1]Developmental Neurogenomics Unit, National Institute of Mental Health, NIH, Bethesda, MD, USA.

[2]Department of Physiology, Anatomy and Genetics, Oxford University, UK.

[3]Vagelos College of Physicians and Surgeons, New York, NY, USA.

[4]Department of Psychiatry, Cambridge University, Cambridge, UK.

[5]Department of Biostatistics, Epidemiology, and Informatics, University of Pennsylvania, Philadelphia, PA 19104, USA.

[6]Cerebral Imaging Center, Douglas Mental Health University Institute, Montreal, Quebec, Canada.

[7]Department of Biological and Biomedical Engineering, McGill University, Montreal, Quebec, Canada.

[8]Schulich School of Medicine and Dentistry, Western University, London, Ontario, Canada.

[9]Department of Psychiatry, Yale University, New Haven, CT, USA.

[10]Department of Psychiatry, University of California–San Diego, La Jolla, CA, USA.

[11]Department of Psychiatry, University of Pennsylvania, Philadelphia, PA 19104, USA.

[12]Mouse Imaging Center, Hospital for Sick Children, Toronto, ON, Canada.

Abstract

Brain size variation over primate evolution and human development is associated with shifts in the proportions of different brain regions. Individual brain size can vary almost twofold among typically developing humans, but the consequences of this for brain organization remain poorly understood. Using in vivo neuroimaging data from more than 3000 individuals, we find that larger

† Corresponding author. raznahana@mail.nih.gov.

Author contributions: Conceptualization, P.K.R. and A.R.; Methodology, all; Software, R.P., M.T.M.P., J.P.L., and M.M.C.; Investigation and Visualization, P.K.R., S.L., J.S., and A.R.; Resources, S.V., A.A.-B., L.S.C., J.D.B., F.M.L., R.C.G., R.E.G., T.D.S., and R.T.S.; Writing, all.

*These authors contributed equally to this work.

Competing interests: None declared.

Data and materials availability: PNC, Genotypes and Phenotypes (dbGaP accession phs000607.v2. p2). NIH, Data available on request through A.R. HCP, S1200 release from humanconnectome.org. Scaling maps presented in this manuscript are available for download at https://neurovault.org.

human brains show greater areal expansion in distributed frontoparietal cortical networks and related subcortical regions than in limbic, sensory, and motor systems. This areal redistribution recapitulates cortical remodeling across evolution, manifests by early childhood in humans, and is linked to multiple markers of heightened metabolic cost and neuronal connectivity. Thus, human brain shape is systematically coupled to naturally occurring variations in brain size through a scaling map that integrates spatiotemporally diverse aspects of neurobiology.

Total brain size can vary almost twofold among typically developing humans of the same age (1). Brain size variation has been linked to coordinated changes in the proportional size of different brain systems across primate evolution and development (2), but the relationship between interindividual variation in human brain size and brain shape remains less well understood (3). We mapped this relationship at high spatial resolution to identify organizational shifts accompanying human brain size variation and illuminate differential areal patterning in larger versus smaller brains.

Our study included 2904 structural magnetic resonance imaging brain scans from two independent primary cohorts: (i) a Philadelphia Neurodevelopmental Cohort (PNC) sample of 1373 cross-sectional scans from a 3 Tesla machine in youth aged 8 to 23 years (table S1A and fig. S1A) (4) and (ii) a National Institutes of Health (NIH) sample of 1531 longitudinally acquired brain scans from a 1.5 Tesla machine in 792 youth aged 5 to 25 years (table S1B and fig. S1B) (1). To generate a reference map of areal scaling in the cortex, we measured the local surface area associated with each of ~80,000 cortical points per scan (henceforth “vertex area”) using an automated image-processing pipeline (5) and then used semiparametric generalized additive models (6) to estimate vertex-specific scaling as the log-log regression coefficient for total cortical area as a predictor of vertex area (Methods). Within this regression framework (7), a coefficient of 1 indicates linear scaling (e.g., doubling of vertex area with a doubling of cortical area), whereas deviation from 1 indicates nonlinear scaling: Coefficients >1 indicate that proportional vertex area increases with greater cortical size (“positive scaling”), and coefficients <1 indicate that proportional vertex area decreases (“negative scaling”). The models used to estimate scaling coefficients provided statistical control for age and sex effects on vertex area, after first ruling out statistically significant interactions between either of these variables and total cortical area (Methods). Thus, our results supported estimation of a single scaling map for each of the two developmental cohorts examined, which did not vary as a function of age and sex.

In both cohorts, scaling relationships between vertex area and total cortical area varied across the cortical sheet (Fig. 1A) in a manner that was broadly symmetric (but see fig. S2 for exceptions) and reproducible in the adult subset of each cohort (Methods, fig. S3A, and table S2). Intervertex differences in scaling were highly correlated between PNC and NIH cohorts (Pearson $r = 0.7$), at levels above chance in a spatial permutation procedure that relies on random surface-based rotation of cortical maps (henceforth “spins”; i.e., $p_{SPIN} < 0.001$) (Methods, Fig. 1A, and table S2). Testing for statistically significant deviation from 1 of vertex scaling coefficients and correcting for multiple comparisons across vertices (Methods) defined two distributed domains of statistically significant, nonlinear areal scaling in each cohort (Fig. 1B). Across cohorts, we observed regions of positive areal scaling in

prefrontal, lateral temporoparietal, and medial parietal cortex, and negative areal scaling in limbic, primary visual, and primary sensorimotor regions (Fig. 1C). The reproducibility of areal scaling across cohorts was unlikely to reflect intrinsic methodological artifacts from a shared cortical analysis pipeline (5) because these scaling patterns were (i) lost after permuting scans across individuals in the PNC cohort (fig. S3B and table S2) and (ii) seen after processing a third independent magnetic resonance imaging (MRI) dataset from the Human Connectome Project (HCP) (n = 1113) (Methods) with a different computational pipeline (FreeSurfer, Methods), at varying smoothing kernels (Fig. 1D, fig. S4, and table S2). Thus, log-log regression analysis revealed regionally specific patterns of nonlinear areal scaling in the human cortex that were broadly reproducible across three study cohorts, three image-acquisition platforms, two image processing pipelines, and a range of smoothing kernels.

To complement log-log regression analysis of scaling, we also generated person-level measures of cortical proportionality by expressing vertex area estimates as proportions of the total cortical surface area in each scan. Variability in proportional vertex area differed across the cortical sheet (fig. S5A), and maps for the relationship between proportional vertex area and total cortical area (fig. S5B) recapitulated the scaling gradients detected by log-log regression (Fig. 1A). Across individuals, raw surface area within regions of positive and negative scaling (Fig. 1B) increased with total cortical size, whereas the total proportional areas of these regions were positively and negatively (respectively) related to total cortical area (Fig. 1E). The ratio between mean proportional vertex area in regions of positive versus negative scaling–a summary “scaling index” that could be computed for each scan–showed a robust positive linear relationship with total cortical area in both cohorts (fig. S5C) and a positive relationship with measures of intelligence quotient (IQ) that were available for the NIH cohort (P = 0.004) (Methods, Fig. 1F, and table S3). However, scaling index variation predicted a small fraction of IQ variance (~1%), and this association did not survive correction for total cortical size (Methods, Fig. 1F, and table S3), which was itself more robustly associated with IQ (see standardized coefficients and model R^2, table S3). Thus, mounting cortical size was simultaneously associated with a greater scaling index and IQ, but differences in scaling above and beyond those predicted by cortical size did not explain additional variance in IQ.

To assess whether regional differences in areal scaling were specific to the cortical sheet, we mapped areal scaling across five non-neocortical (henceforth “subcortical”) structures (thalamus, pallidum, striatum, hippocampus, and amygdala) using recently developed algorithms for automated subcortical shape analysis (MAGeT Brain, Methods). This approach provided a homogeneous surface-based framework for quantification and visualization of areal scaling gradients across the cortex and subcortex (Methods, fig. S6, A and B). Vertex-level areal scaling coefficients varied within each subcortical structure examined (e.g., positive scaling in hippocampal head versus negative scaling in tail) (fig. S6C), revealing that size-related shifts in human brain shape are not restricted to the neocortex.

To assess the biological importance of spatially patterned areal scaling within the human brain, we compared regional differences in cortical scaling to several independent assays of

cortical organization. We first investigated whether patterns of cortical area redistribution as a function of normative brain size variation in humans (Fig. 1A) aligned with those that accompany evolutionary and developmental changes in primate brain size (Fig. 2, A to D) (2). Intervertex scaling variations in PNC and NIH cohorts (Fig. 1A) were positively correlated with those seen in evolution and development (Fig. 2, A to C, and table S2). All three sources of primate brain size disparity (evolution, development, and naturally occurring size variation) involved disproportionate areal expansion within anterior cingulate, angular gyrus, superior parietal lobule, and lateral temporal cortex (Fig. 2, B and D). Within these regions, the magnitude of positive areal scaling between macaques and humans tended to exceed that seen within humans (fig. S7A).

We next asked whether regional differences in human cortical scaling were related to functional and microstructural topography of the human cortex. Using a previously published parcellation of the cortical sheet into seven canonical resting-state functional connectivity networks (8), we found that (i) regions of positive scaling were concentrated within association cortices, including the default mode (DMN), dorsal attention, and frontoparietal networks ($p_{SPIN} = 0.001$ for DMN), whereas (ii) regions of negative scaling were overrepresented ($p_{SPIN} = 0.007$) within the limbic network (Fig. 2E and table S4). These associations were replicated using a finer-grained functional parcellation of the human cortex (8) (fig. S7B and table S4), and indicated that larger human brains show preferential areal expansion within regions of association cortex that sit at the apex of a functional network hierarchy (9,10) and provide high-level integration across lower systems (11). This theme was reinforced by comparison of scaling maps with a classical parcellation of the cortex into seven cytoarchitectonic “types” with differing laminar organizations (12): Regions of positive areal scaling were overrepresented within “von Economo Type 3” cortices (Fig. 2F and table S4) that bear cytoarchitectonic specializations for long-range cortico-cortical connectivity (e.g., thickening of supragranular layers II/III). Thus, regions of preferential areal expansion in larger versus smaller human brains appeared to be both functionally and microstructurally suited to operate as hubs of information integration.

To next probe potential molecular correlates of regional differences in cortical scaling, we used a shared stereotaxic coordinate system to assign an areal scaling coefficient (Fig. 1A) to each of 1939 spatially distributed and transcriptomically characterized cortical samples from an independent cohort of six adult human donors provided by the Allen Institute for Brain Science (AIBS) (13) (Methods, Fig. 3A, and table S5). This data alignment allowed us to rank ~16,000 genes by the spatial correspondence between their expression and cortical scaling gradients in PNC and NIH cohorts (Methods, table S6), with expression of the high-ranking genes being most positively correlated with scaling (Fig. 3B). Rank-based gene ontology (GO) analysis (Methods) (14) revealed that high-ranking genes were significantly enriched for mitochondrial and synaptic GO annotations (Fig. 3C) and related processes of oxidative phosphorylation and transmembrane K^+ transport (table S7). Observed gene ranks were robust to randomly excluding up to 70% of samples per donor, and the high rank of genes associated with mitochondrial and synaptic GO terms was lost after permutation of scaling values across AIBS samples (Methods). The positive association between areal scaling and postmortem expression of mitochondria-related genes (Fig. 3C and table S7) suggested that cortical regions that are preferentially expanded in larger versus smaller

human brains may possess a distinct energy metabolism profile. This hypothesis was supported by convergent evidence for a statistically significant positive association between regional differences in cortical areal scaling and regional differences in two different neuroimaging proxies for cortical energy consumption at rest (15,16) (Fig. 3D and table S2).

Our findings illuminate several aspects of cortical patterning. First, the spatial convergence of areal scaling maps across all three major axes of primate brain size variation (Fig. 2)–evolution, development, and standing interindividual variation–implies shared mechanisms for size-dependent patterning of the primate cortical sheet. These mechanisms presumably link variation in early progenitor cell proliferation to (i) the genesis of regional differences in cellular composition during prenatal corticogenesis (17,18) or (ii) the subsequent emergence of regional differences in cellular morphology and neuropil composition (19) Second, the anabolic costs of tissue growth (20) and the overlap of positive areal scaling with diverse markers of biological investment (Fig. 3) suggest that preferential expansion of association cortex (e.g., DMN) may serve to maintain or enhance (21) brain function in larger versus smaller human brains. Testing this hypothesis will require new study designs that can probe diverse assays of human brain function beyond IQ while untangling the effects of brain size variation from linked changes in cortical patterning (Fig. 1F). Finally, the convergent evidence that cortical regions of positive scaling are specialized for integration of information across lower-order systems (Figs. 2 and 3) offers a potential mechanistic account for positive areal scaling in the primate brain. Just as the computational load of an integrative algorithm can increase supralinearly with the size of its inputs (22), larger cortices may need to disproportionately expand the anatomical substrates for integrative computation in association cortex. Based on our results (Figs. 2F and 3C) and available comparative histology (23), we speculate that these substrates include dendritic branching and synaptic spine density in supragranular neuropil.

In summary, naturally occurring variations in human brain size are accompanied by systematic changes in brain shape through scaling gradients that tie together macroscopic, microscopic, and evolutionary features of the human brain.

Supplementary Material

Refer to Web version on PubMed Central for supplementary material.

ACKNOWLEDGMENTS

The authors thank all research volunteers within the cohorts studied for their participation and all the reviewers for their helpful comments. A.R. thanks SVR and AIR for their support.

Funding: This research was partially funded by the NIMH Intramural (ZIA MH002794, PI A.R.) and Extramural (R01MH107235, R01NS085211, R01NS060910, R01MH112847, and R01MH107703, PIs S.V., R.C.G., R.E.G., T.D.S., and R.T.S.) Research Programs. Data were provided in part by the Human Connectome Project, WU-Minn Consortium (PIs: David Van Essen and Kamil Ugurbil; 1U54MH091657) funded by the 16 NIH Institutes and Centers that support the NIH Blueprint for Neuroscience Research; and by the McDonnell Center for Systems Neuroscience at Washington University.

REFERENCES AND NOTES

1. Giedd JN et al., Neuropsychopharmacology 40, 43–49 (2015). [PubMed: 25195638]

2. Hill J. et al., Proc. Natl. Acad. Sci. U.S.A. 107,13135–13140 (2010). [PubMed: 20624964]
3. Mankiw C. et al., J. Neurosci. 37, 5221–5231 (2017). [PubMed: 28314818]
4. Satterthwaite TD et al., Neuroimage 86, 544–553 (2014). [PubMed: 23921101]
5. Ad-Dab'bagh Y. et al., The CIVET image-processing environment: A fully automated comprehensive pipeline for anatomical neuroimaging research. Proceedings of the 12th Annual Meeting of the Organization for Human Brain Mapping (2006).
6. Stasinopoulos M, Biometrics 63, 1298–1299 (2007).
7. Huxley J, Nature 114, 895–896 (1924).
8. Yeo BTT et al., J. Neurophysiol. 106, 1125–1165 (2011). [PubMed: 21653723]
9. Sporns O, Curr. Opin. Neurobiol. 23, 162–171 (2013). [PubMed: 23294553]
10. Margulies DS et al., Proc. Natl. Acad. Sci. U.S.A. 113, 12574–12579 (2016). [PubMed: 27791099]
11. Medaglia JD, Lynall M-E, Bassett DS, J. Cogn. Neurosci. 27, 1471–1491 (2015). [PubMed: 25803596]
12. von Economo CF, Koskinas GN, Die Cytoarchitektonik der Hirnrinde des Erwachsenen Menschen (J. Springer, 1925).
13. Hawrylycz MJ et al., Nature 489, 391–399 (2012). [PubMed: 22996553]
14. Eden E, Navon R, Steinfeld I, Lipson D, Yakhini Z, BMC Bioinformatics 10, 48 (2009). [PubMed: 19192299]
15. Satterthwaite TD et al., Proc. Natl. Acad. Sci. U.S.A. 111, 8643–8648 (2014). [PubMed: 24912164]
16. Glasser MF, Goyal MS, Preuss TM, Raichle ME, Van Essen DC, Neuroimage 93, 165–175 (2014). [PubMed: 23567887]
17. Reillo I, de Juan Romero C, García-Cabezas MÁ, Borrell V, Cereb. Cortex 21, 1674–1694 (2011). [PubMed: 21127018]
18. Cahalane DJ, Charvet CJ, Finlay BL, Front. Neuroanat. 6, 28 (2012). [PubMed: 22826696]
19. Elston GN, Fujita I, Front. Neuroanat. 8, 78 (2014). [PubMed: 25161611]
20. Kuzawa CW et al., Proc. Natl. Acad. Sci. U.S.A. 111, 13010–13015 (2014). [PubMed: 25157149]
21. Rubinov M, Nat. Commun. 7, 13812 (2016). [PubMed: 27924867]
22. Sipser M, Introduction to the Theory of Computation (Thompson Course Technology, ed. 2, 2006).
23. Elston GN, Cereb. Cortex 13, 1124–1138 (2003). [PubMed: 14576205]

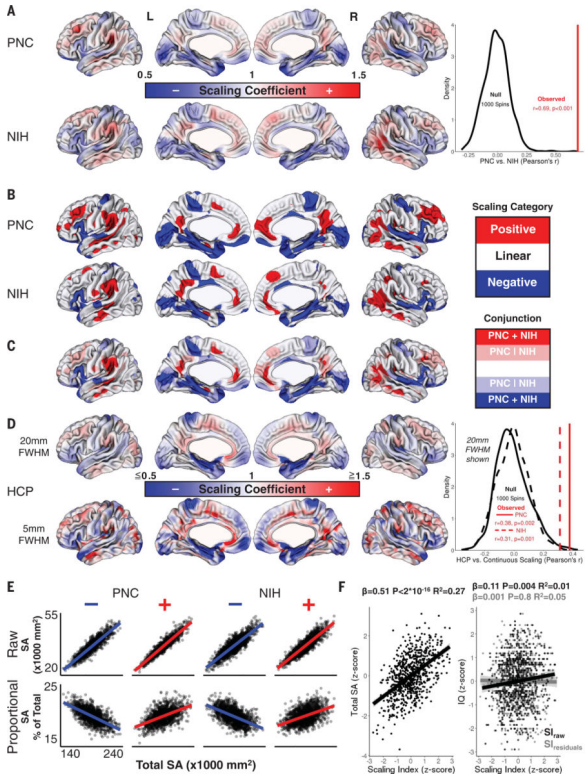

Fig. 1. Nonlinear areal scaling of the cortex with normative brain size variation in PNC, NIH, and HCP cohorts.

(A) Unthresholded vertex maps showing local surface area scaling with naturally occurring variations in total cortical area. Red, relative expansion in larger cortices ("positive scaling"); blue, relative contraction ("negative scaling"). The observed cross-vertex correlation in scaling between PNC/NIH cohorts is greater than that in 1000 surface-based rotations of the NIH scaling map (i.e., $p_{SPIN} < 0.001$, density plot). (**B**) Categorical scaling maps showing regions of statistically significant positive and negative areal scaling (i.e., H_o: scaling coefficient = 1 rejected) after correction for multiple comparisons across vertices. (**C**) Conjunction of PNC and NIH maps from Fig. 1B. (**D**) Regional scaling in a third independent dataset (Human Connectome Project, $n = 1113$), across two different FWHM (full width at half maximum) smoothing kernels (for maps for all five kernels, see fig. S4). Density plot shows that observed alignment of HCP scaling with PNC (solid)/NIH (dashed) ($r > 0.3$) exceeds chance ($p_{SPIN} < 0.002$). (**E**) Scatter plots of raw (top row) and proportional (bottom row) surface area in regions of nonlinear scaling from Fig. 1B versus total cortical area (SA). (**F**) Inter-relationships between age and sex residualized scaling index (SI, with and without residualization for SA), SA, and IQ in the NIH cohort.

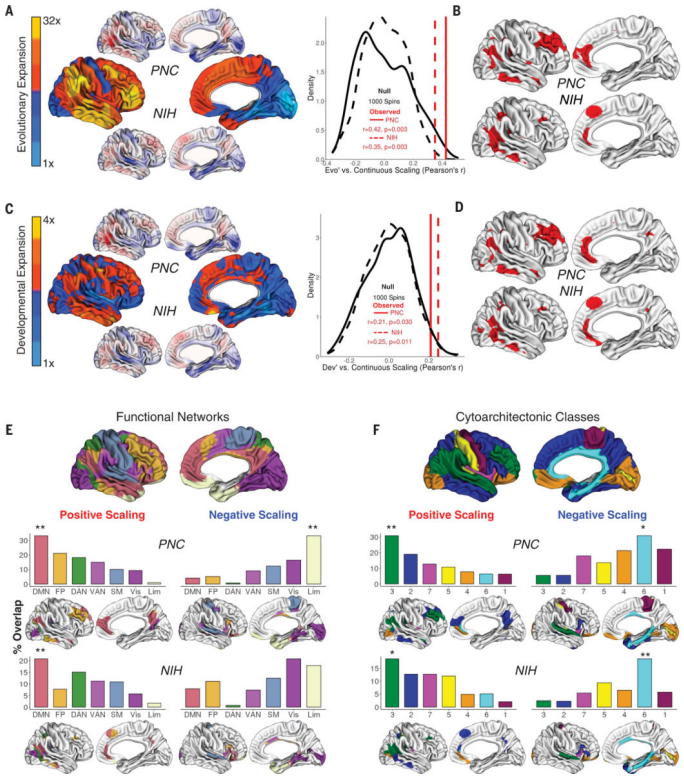

Fig. 2. Areal scaling aligns with patterns of cortical evolution, development, functional network topography, and cytoarchitecture.

(A) Area expansion map in humans relative to macaques (2), with PNC/NIH scaling maps for comparison. Density plot shows that observed spatial correlation of scaling maps and evolutionary expansion is greater than chance for PNC (solid) and NIH (dashed) cohorts. (**B**) Conjunction between regions of positive areal scaling in PNC/NIH cohorts (Fig. 1B) and vertices with evolutionary expansion values above the 50th centile. (**C** and **D**) Identical analyses as Fig. 2, A and B, except for areal expansion map in human adults relative to human infants (2). (**E**) Parcellation of cortex into seven canonical resting state functional connectivity networks (8), with bar plots and conjunction maps showing differential representation of positive versus negative scaling in each network (** $p_{SPIN} < 0.001$, * $p_{SPIN} < 0.05$). Regions of positive scaling localize to the default mode network (DMN) and regions of negative scaling to the limbic network (Lim). (**F**) Cortical parcellation into seven different laminar types according to a classical cytoarchitectonic atlas (12), with bar plots and conjunction maps showing that regions of positive scaling localize to von Economo Type 3 cortex, and negative to Type 6 (** $p_{SPIN} < 0.001$, * $p_{SPIN} < 0.05$).

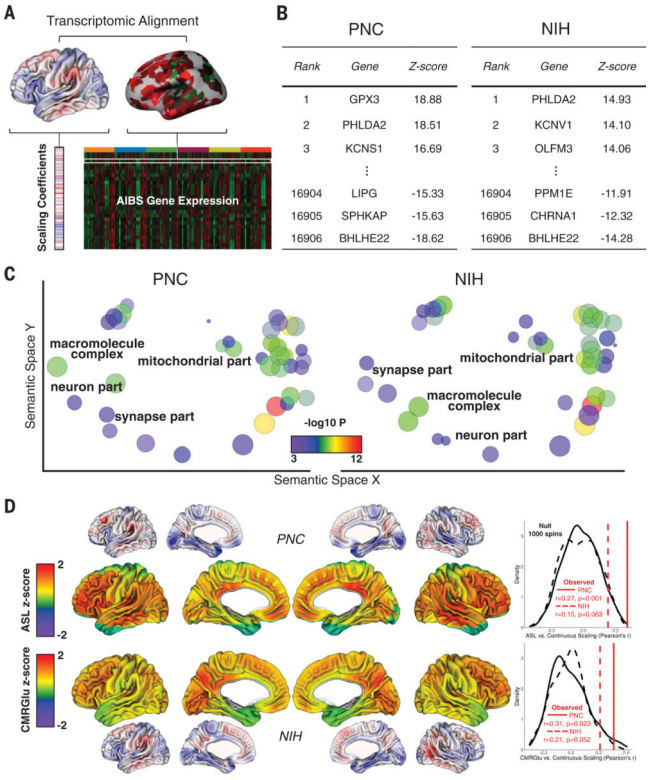

Fig. 3. Areal scaling aligns with cortical gene expression and metabolism.

(A) Vertex scaling coefficients from PNC and NIH maps (Fig. 1A) were uniquely assigned to each of ~2k cortical samples from the Allen Institute for Brain Sciences (AIBS) (13) by spatial proximity, allowing ranking of the ~16,000 genes measured across all AIBS samples by their spatial correlation with areal scaling. (**B**) Extreme-ranking genes for the PNC and NIH scaling maps. (**C**) Visualization of GO cellular component terms in semantic space showing statistically significant enrichment of mitochondria- and synapse-related terms among top-ranking genes. (**D**) Areal scaling is positively correlated with two neuroimaging-based proxies for cortical energy consumption at rest: arterial spin labeling (ASL) measures of arterial blood flow (15) and positron emission tomography measures of glucose uptake (CMRGlu) (16) (density plots, PNC solid, NIH dashed, black null, red observed, mean $p_{SPIN} < 0.03$).